Observations of short period seismic scattered waves by small seismic arrays

Edoardo Del Pezzo([1]), **Mario La Rocca**([2]), **Rosalba Maresca and Maria Simini**([2])
([1]) *Dipartimento di Fisica, Università di Salerno, Italy*
([2]) *Dipartimento di Geofisica e Vulcanologia, Università di Napoli «Federico II», Napoli, Italy*

Abstract
The most recent observations of well correlated seismic phases in the high frequency coda of local earthquakes recorded throughout the world are reported. In particular the main results, obtained on two active volcanoes, Teide and Deception, using small array are described. The ZLC (Zero Lag Cross-correlation) method and polarization analysis have been applied to the data in order to distinguish the main phases in the recorded seismograms and their azimuths and apparent velocities. The results obtained at the Teide volcano demonstrate that the uncorrelated part of the seismograms may be produced by multiple scattering from randomly distributed heterogeneity, while the well correlated part, showing *SH* type polarization or the possible presence of Rayleigh surface waves, may be generated by single scattering by strong scatterers. At the Deception Volcano strong scattering, strongly focused in a precise direction, is deduced from the data. In that case, all the coda radiation is composed of surface waves.

Key words *scattering – arrays*

1. Introduction

The seismic coda, or the end portion of high frequency seismograms, is generally interpreted as produced by scattering phenomena in the crust (Aki, 1995; Hoshiba, 1995). There have been many theories of coda wave generation. The most important are the single scattering theory (Aki and Chouet, 1975; Sato, 1977), the multiple scattering theory (Gao *et al.* 1983), the energy transport theory (Wu and Aki, 1985) and the energy flux theory (Frankel and Wennerberg, 1987). For simplicity, application of the above mentioned models uses the hypothesis of spatial uniformity of scattering and absorption, but it is reasonable, and widely accepted, that the earth medium in which the scattering phenomena occur is far from being uniform. In fact many experimental results have been interpreted as a demonstration that the seismic wave attenuation decreases with depth (Gagnepain Beyneix, 1987), showing that at least at regional scale, some heterogeneity exists in the lithosphere. Due to this observational evidence, the methods based on the use of coda waves under the hypothesis of a uniform medium lead to questionable results. Attempts have been made to use non-uniform media in the model of multiple scattering (Hoshiba, 1994, 1995) in order to re-interpret the results obtained under the assumption of uniformity, but it remains necessary, to avoid

Mailing address: Prof. Edoardo Del Pezzo, Dipartimento di Fisica, Università di Salerno, 84081 Baronissi (SA), Italy; e-mail: delpezzo@vaxsa.csied.unisa.it

uncertainties, to experimentally observe the heterogeneity of the earth medium in order to apply the correct scattering model.

This last objective can be reached using data from seismometer arrays. Array techniques, applied to the whole seismogram, are able to furnish the slowness and apparent velocity of the seismic, «phases» that compose the coda portion. In this way it is possible to obtain information on the location of possible «strong scatterers» which contribute to the coda formation. At present, results are few, due to the experimental difficulty of finding well correlated phases in the coda, even though presumably the observations will increase in the near future given the rapidly increasing diffusion of the portable seismic instrumentation.

The aim of the present paper is to report the most recent observations of well correlated scattered waves in the high frequency coda of local earthquakes recorded throughout the world. These observations allow the investigation of the space distribution of the scatterers which contribute to the formation of the coda of small magnitude local earthquakes. In particular, we describe the main results obtained by our and other Europen research groups, using small arrays on two active volcanoes.

2. Review of the most recent main results

Scattered short period (0.3-1.5 Hz) body waves were observed in the *P*-coda of several teleseisms recorded at LASA array by Aki (1973). This author first pointed out the possibility of interpreting the variation of amplitude and travel time with respect to a uniform earth model beneath the LASA array with the presence of randomly distributed scatterers, in a statistically homogeneous and isotropic medium. Aki (1973) found an average correlation distance of 10 km and a scattering coefficient of 0.008 km^{-1} under LASA. Moreover this author demonstrated that, at least for the frequency of 0.5 Hz, the scattering is so strong as to violate the Born approximation. This result also contributed to the development of the single scattering model for coda generation (Aki and Chouet, 1975) which has been widely used to estimate the average gross properties of the Earth's crust and upper lithosphere in many zones of the world.

P wave packets from local earthquakes recorded at a small aperture array located at Pinyon Flat, California, were used to study the coherence of the wave field in the frequency band from 1 to 50 Hz (Vernon *et al.*, 1991). These authors obtained the important result that at 500 m station separation the body waves are incoherent above 15 Hz. Moreover, it was demonstrated that a random velocity distribution is necessary with standard deviation higher than 10% to explain the observed results. As the Pinyon array was set up in a site of homogeneous granitic geology and planar topography, practically a site which could be defined as a hard rock site, this result strongly constrains all the observations of high frequency seismogram at arrays with aperture as small as some hundredths of meters.

A large array (inter-distances of the order of 5-10 km) was used by Nishigami (1991) to determine the spatial distribution of the scatterers producing the *S*-wave scattering field. This author finds strong localized scatterers producing the main energy bursts in the coda of local earthquakes at a depth of 4-24 km, with some correlation with the main active faults in the investigated zone (Central Japan). The perturbation of the scattering coefficient was estimated to be about 20% and in the hypothesis that the scattering is mainly produced by velocity fluctuations Nishigami (1991) finds that the velocity fluctuation in the fault zones is more than 10% larger than the average.

At regional scale Dainty and Toksoz (1990) applied frequency-wavenumber analysis to regional earthquake data from the array NORESS, FINESA and ARCESS. For regional seismograms, they found *Lg* to *Lg* forward scattered phases in the early coda, and isotropic back-scattering in the late coda.

Frankel *et al.* (1991), using records from a small array in Sunnyvale (CA), showed that the coda of local earthquakes is composed mostly of surface waves with almost random back-azimuths and an apparent velocity which decreases with increasing lapse time along the coda.

Spudich and Botswick (1987), applying the principle of reciprocity to an array of microearthquakes, showed that the early *S*-coda at Morgan hill region, California is dominated by a persistent signal that must be caused by multiple scattering, possibly within 2 km of each station. The late *S*-coda is different from the early coda, decaying more regularly with almost no dependence on the site.

Goldstein and Chouet (1994) applied array analysis to data from Kilauea volcano, Hawaii, showing that tremor and volcanic earthquakes generated by the gas piston mechanism consist of a complex combination of body and surface waves. In the late coda of gas piston events the signal maintains high correlation and the array analysis shows a quite constant ray parameter along the seismogram. Chouet *et al.* (1997) applied array analysis to explosion quakes at Stromboli volcano, Italy, showing possible near site strong scatterers in the early coda, and a complex surface wave composition of the coda waves. As in the case of Kilauea volcano, the pattern of ray parameters as a function of lapse time along the coda of the Stromboli quakes shows that a significant part of the scattered waves is focused in the source-array direction.

Summarizing the above observations, it can be said that:

a) The *P*-coda is dominated by forward scattering at low frequency (around 1 Hz).

b) The distribution of the scatterers in the crust can be described by an average correlation distance of 10 km in stable zones; in tectonically active zones the presence of faults perturbs the scattered wave field.

c) The correlation among the array stations is good up to an inter-station distance of no more than 500 m.

d) The unstable zones, like for example the active volcanic or tectonic areas, show the presence of surface waves in the coda, indicating possible strong scatterers located at the surface.

e) For seismic events generated on volcanoes, due to the persistency of the seismic source associated to the volcanic phenomena, most of the scattered wave field is focused in the source-array direction.

3. Results obtained and methods applied by the present authors

In this section we will report the most recent, only partly published results obtained by some of the present authors using two small arrays of short period seismometers which were set up on two active volcanoes, the Teide volcano in Canary Island and Deception volcano located in Antarctica. The aim of these two seismic surveys was seismic monitoring, but in both cases the data were used to study late arrivals along the seismogram. In particular, the total *S*-coda radiation between the *S*-wave arrival and the end of the seismogram, was studied for the data recorded on Teide volcano. At Deception, the data showed the absence of high energy shear wave signals, and indicated a strong presence in the coda of surface waves. In both cases the array analysis gives some useful information about the secondary wave composition of the short period seismograms. An array method based on the measurement of the zero-lag cross-correlation was developed and applied in both cases, allowing the study of secondary seismic phases with a very short time duration.

4. The method

In the hypothesis of a plane wave across a two-dimensional array of seismic stations (set up in a flat zone) with an apparent slowness vector $\boldsymbol{p} \equiv (p_x, p_y)$, let t_{ij} be the travel time difference between the stations i and j of the array. Then

$$t_{ij} = p_x \, \Delta x_{ij} + p_y \, \Delta y_{ij}.$$

where p_x and p_y are the Cartesian components of the apparent slowness vector, and Δx_{ij}, Δy_{ij} are the differences between the coordinates of the stations i and j. If the seismic traces are time-shifted by t_{rj} measured with respect to a reference station, r, then the Zero Lag Cross-

correlation (ZLC) coefficient (Frankel *et al.*, 1991), given by

$$c_{i,j} = \frac{\sum_{k=1}^{M} A_k^i \cdot A_k^j}{\sqrt{\sum_{k=1}^{M} (A_k^i)^2 \cdot (A_k^i)^2}}$$

where A are seismogram amplitudes, k is the time sample and M the number of time samples, is maximum for each pair of stations i, j. It is clear that $c_{ij} = c_{ji}$. Thus, if we have N seismograms $N(N-1)/2$ different values of c_{ij} will exist. Also, the average of all the coefficients c_{ij}, $\langle c_{ij} \rangle$, will be maximum.

A grid search is then used to find, for each earthquake recorded at the array of stations, the apparent slowness vector which maximizes $\langle c_{ij} \rangle$. The procedure is described briefly in the next 6 steps:

1) We fix the value of the apparent slowness on a grid, in the range from 1/500 to 1/15000 s/m.

2) We calculate the corresponding set of t_{rj} and then we shift the seismograms.

3) We calculate the zero-lag cross-correlation for each station pair and then the average.

4) We repeat the cycle starting again from step 1; in this way we obtain the average zero lag cross-correlation $c(p_x, p_y)$ for all the values of the slowness fixed on the grid.

5) We select the maximum of $c(p_x, p_y)$ which will correspond to the «true» slowness vector.

6) The back-azimuth is obtained by the formula $\phi = \arctan(p_x/p_y)$, and the apparent velocity by $v_a = 1/(p_x^2 + p_y^2)^{0.5}$.

In Del Pezzo *et al.* (1997) more details about this methods are reported together with a block scheme of the entire procedure.

It is noteworthy that if the grid is obtained using constant Δp increments, the resolution decreases for increasing apparent velocities. To avoid this effect we increment $\phi = \arctan(p_x/p_y)$ by a constant quantity $\Delta\phi$; $p = (p_x^2 + p_y^2)^{0.5}$ was incremented by Δp in such way that $\Delta p/p$ remains constant. In this way we obtain a good compromise between resolution and computer speed. A similar procedure was also used by Frankel *et al.* (1991) and by Mori *et al.* (1994). The errors on the estimates of the back-azimuths and slowness depend on the signal to noise ratio, space and time sampling of the wavefield and on the grid spacing. The full description of the method used to evaluate them is reported in Del Pezzo *et al.* (1997). Here, for brevity we do not report this discussion. The maximum errors are of the order of 10% of the estimates for the analysis described in the following two sections.

5. Data analysis and results for Teide volcano

In the framework of TELV (Teide European Laboratory Volcano project, sponsored by European Science Foundation; Arana, 1994) an array of short period seismic stations was set up inside the Teide Caldera with the principal aim of seismic monitoring.

Teide volcano has been quiescent since 1929, and the only manifestation of activity is a fumarole field near the cone. No clear information about the local seismic activity recorded before the time of the present experiment is available.

The array location and configuration are shown in figs. 1 and 2, respectively. The location is a flat area inside the caldera with apparently uniform surface geology, surrounded by strong topographic irregularities, like the two Teide cones (Pico Teide and Pico Viejo) and the caldera rim. We used the array AB for the present analysis.

The data set consists of some tens of small-magnitude local seismic events, recorded in the period September 11, 1994-November 12, 1994. A visual analysis of all the seismic traces which were recorded allowed us to select, for the study of the scattering sources, a subset of 7 earthquakes characterized by clear P and S wave onsets and a regularly decaying coda lasting more than 20 s (see an example in fig. 5). These earthquakes clearly show the features of the tectonic earthquakes, as their amplitude displacement spectra (not reported) show a flat

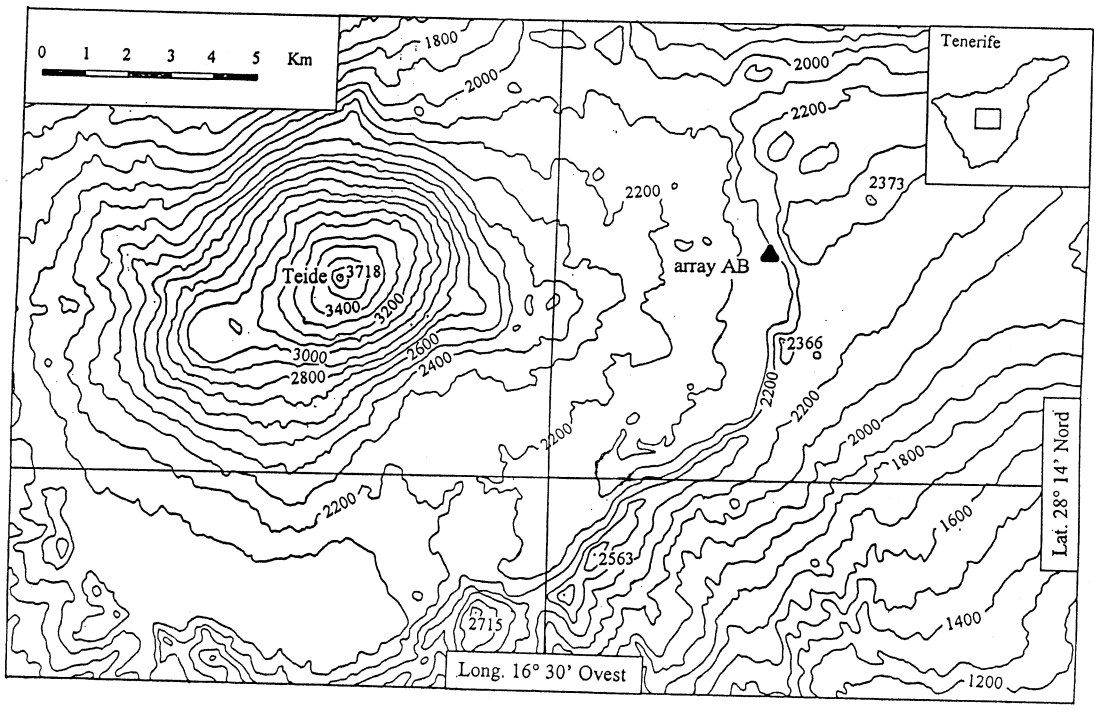

Fig. 1. Topography of Teide volcano area in Tenerife Island (Canary Islands, Spain). The position of the seismic array is indicated with the black triangle.

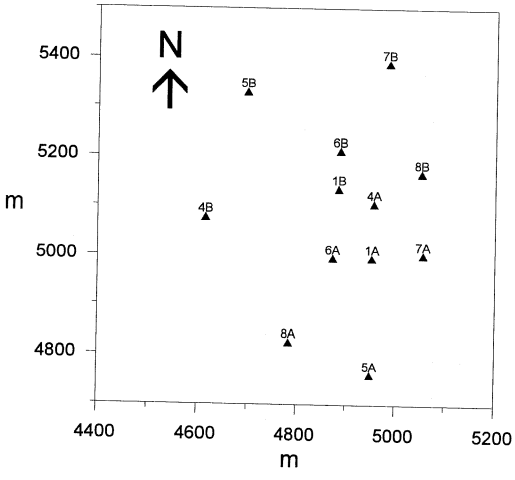

Fig. 2. Configuration of array AB, composed by 10 vertical component sensors and 2 three-component sensors.

portion at low frequency and a rapid high-frequency decay after the corner frequency, differently from what is generally observed for the low-frequency or for explosion quakes which, on the contrary, exhibit more peaked spectra.

The events selected for the present study were firstly band-pass filtered between 4 and 6 Hz, in order to reduce the contamination of low frequency noise due possibly to ocean waves, and high frequency noise which was sometimes produced by wind. A fast spectral analysis carried out on the seismic events reveals that the corner frequencies are always above 6 Hz. The events were located using the *P* and *S* phases recorded at the array AB. We applied the Zero-Lag Cross-correlation (ZLC) method to a windowed (50 samples) portion of the seismograms, centered at the visually determined *P* phase onset, in order to fix the az-

imuth and apparent velocity of the first *P* phase. Then we read visually the *S*-P times at the three component stations of the array, taking the average, and thus we estimated the hypocentral distance, along the ray-path, for a V_p/V_s ratio equal to 1.7. Finally, using a simple ray-tracing procedure based on a flat layered model, we drew the ray connecting hypocenter and array center. In this way we obtained the location of the 7 events selected for the coda study reported in fig. 3. The errors on the slowness components and the uncertainty in the *S-P* reading, of the order of 0.2 s, produce the ellipsoidal uncertainty zone for the epicentral estimate, drawn in fig. 3. The estimate of hypocentral depth (not reported in fig. 3) is largely approximate, due to the fact that the true velocity model is unknown. In the present paper we utilized a «reasonable» model, an average among the velocity models reported in the literature for volcanic areas. The maximum hypocentral depth was about 26 km for the event 2601203, the farthest from the array AB, while the minimum about 2 km for the event 2630024, the nearest.

To study the characteristics of the coda waves, we applied the ZLC method to the whole seismogram, from the first *P* onset to the end of the coda (signal to noise ratio less than 2) in the following way:

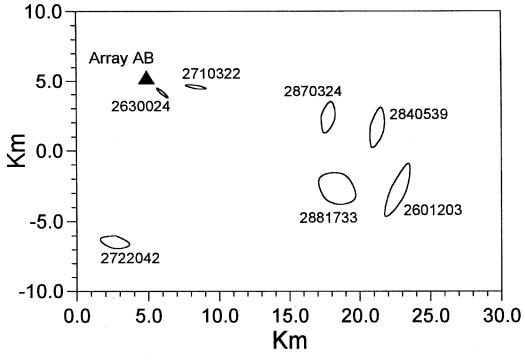

Fig. 3. Location of the seismic sources of the seven earthquakes used for the analysis. These sources were located with ray-tracing techniques by using a flat layered model.

1) We used time windows of 50 samples sliding 30%. For each window we evaluated the maximum correlation and hence the back azimuth and apparent velocity.

2) We «filtered» the data set by discarding all back-azimuth and apparent velocity values, for which the value of the average ZLC was lower than 0.7.

This threshold was chosen on the basis of the array analysis of a sample of pure noise recorded at the array. The noise shows a roughly flat ZLC pattern *versus* lapse time with an average around 0.4 and a standard deviation of about 0.1 (see fig. 4). The threshold was so set up at a value which corresponds to the mean plus three times the standard deviation. We call the arrivals with correlation greater than 0.7 «well correlated arrivals». A plot of the values of back-azimuth and apparent velocity as a function of lapse time, shows the phases in the coda wavetrain which could be generated by strong scatterers. An example of the results is reported in fig. 5. The plots clearly show the arrivals of direct impulsive *P* and *S* phases, and some other late «arrivals» which may correspond to strong scatterers. The figure shows that inside the time window corresponding to primary *P* and *S* waves there are only a few points with high correlation with approximately the same back-azimuth. These correspond to the arrivals of direct *P* and *S*, and possibly to a reflected phase less than 1 second before the *S*-wave arrival. Non impulsive sources, like those for example reported by Chouet *et al.* (1997) for Stromboli volcano, showing focused energy in the source-station direction even in the early coda, were not recorded in the present field survey on Teide volcano.

It is also interesting that the values of apparent velocity decrease soon after the first 10 s from the direct *P*-wave arrival, showing low values of the apparent velocity for the well correlated phases of the short period coda. The back-azimuth pattern *vs.* lapse time, on the contrary, is almost random, showing the presence of all possible values of back-azimuth.

The total distribution of back-azimuth and apparent slowness obtained for coda windows is reported in the histograms of fig. 6a,b. We

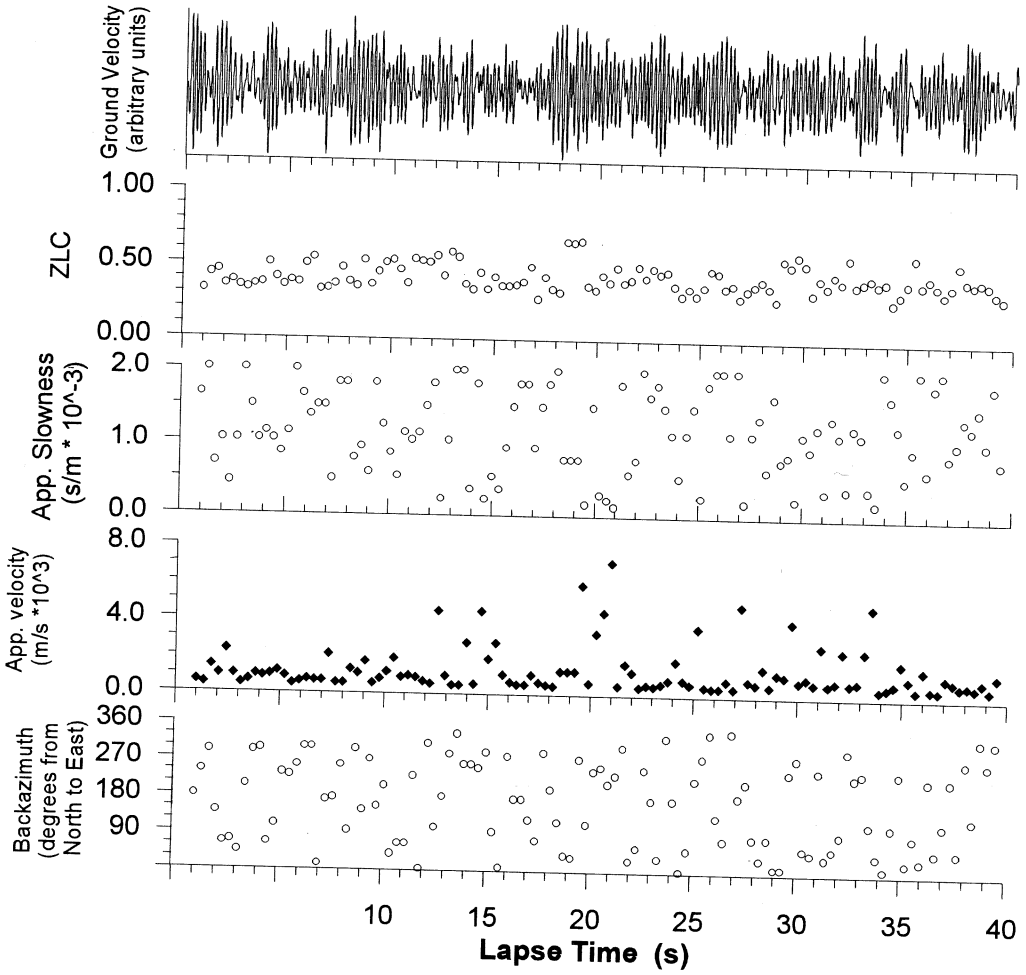

Fig. 4. An example of noise analyzed with the ZLC method using a 50 sample window moving along the signal. For each window are reported: 1) correlation values; 2) slowness vector magnitude; 3) apparent velocity; 4) back-azimuth.

selected the data with values of zero-lag cross-correlation greater than 0.7 and lapse times greater than the *S*-wave travel time. No points were found in the first 3 s after the *S*-wave arrival time. The distribution of the apparent slowness is slightly peaked between about 10^{-3} and 1.6×10^{-3} s/m with a few scattered values between 0.25×10^{-3} and 10^{-3} s/m. The back-azimuths are irregularly distributed between 0 and 360°, showing no significant peaks. These last two figures show that the apparent slowness of the highly correlated phases which compose the coda ranges from values close to the shear wave slowness in the shallowest layers, possibly indicating surface waves, to higher values that could correspond to deep scattering sources.

In order to investigate the composition of the waves that form the coda, we applied a rectilinearity filter (Montalbetti and Kanasevich,

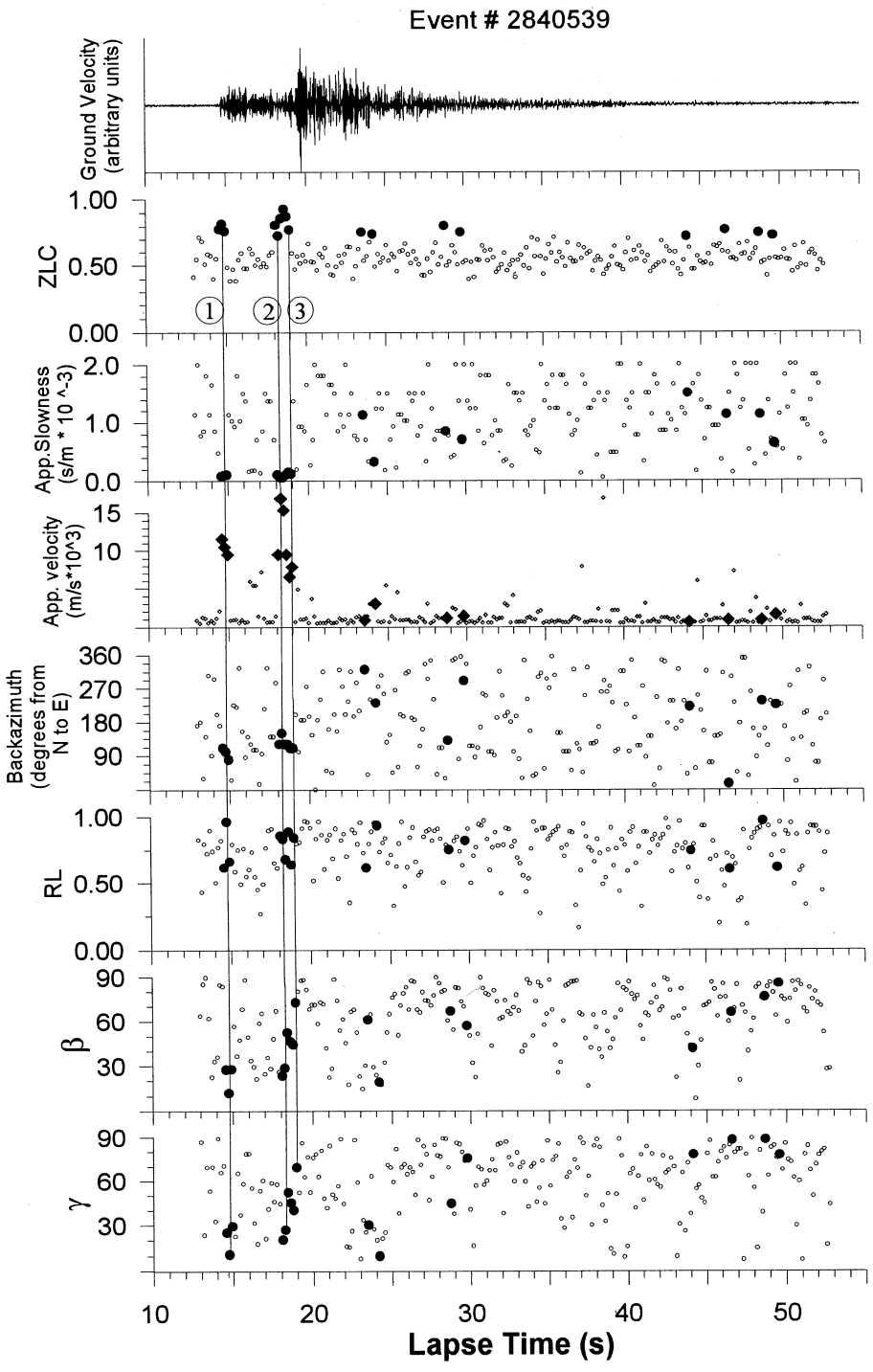
Event # 2840539
Ground Velocity (arbitrary units)
ZLC
1.00
0.50
0.00
1
2
3
App.Slowness (s/m * 10 ^-3)
2.0
1.0
0.0
App. velocity (m/s*10^3)
15
10
Backazimuth (degrees from N to E)
360
270
180
90
RL
1.00
0.50
0.00
β
90
60
30
γ
90
60
30
10
20
30
40
50
Lapse Time (s)

1970) to the whole seismogram of the seven events selected for the array study. We used the station which recorded the best signal to noise ratio of the two 3D stations of the array AB. This filter is based on the evaluation of the coefficient of rectilinearity:

$$R_L = 1 - \lambda_2/\lambda_1$$

where λ_1 and λ_2 are the largest and the next largest one eingenvalues of the covariance matrix of the 3D signal (Montalbetti and Kanasevich, 1970). R_L would be close to unity for high rectilinearity and close to zero for low rectilinearity.

We estimated the direction of polarization by calculating the angle β which the largest eigenvector forms with the vertical at the site, directed downward. If the seismogram is composed of *S*-waves then the direction of polarization must be normal to the wave vector. We estimated the angle which the wave vector forms with the direction of polarization, γ, and plotted it together with β and R_L.

In fig. 5 R_L, β and γ obtained as functions of time, are shown as an example, together with the measured back-azimuths and apparent velocities, for the event 2840539. The data show that on average the rectilinearity is high and that β is close to 80 degrees along the coda, suggesting an average composition of almost horizontally polarized waves. It is interesting to look at the arrivals marked by the vertical lines which correspond to the first phases of the *P* and *S* waves. We observe for the first phase marked by the leftmost vertical line (No. 1) a very high rectilinearity and the lowest values of β and γ, which correspond to a phase with a particle motion parallel to the direction of the wave vector: a compressional phase. Line No. 2 of the same figure shows a phase with high values of rectilinearity and low β and γ, indicating a compressional phase which arrives later than the first at a travel time close to the *S*- wave travel time: probably an *S* converted to *P*. The line No. 3 shows a phase with a high rectilinearity and high β and γ, corresponding to a pure *SH* type wave. In the coda of the seismogram presented as an example in fig. 5 we observe 8 arrivals corresponding to well correlated phases, all with apparent velocity less than 3 km/s and back-azimuths randomly distributed. The rectilinearity, β and γ parameters corresponding to these arrivals are denoted with black dots.

The same observations carried out for the coda time windows of all the events used in the present study show in some cases high rectilinearity with high β and γ, indicating an *SH* composition, while sometimes rectilinearity is lower, around 0.5, with intermediate values of β and γ. In this case the composition may correspond to a Rayleigh type wave. It is noteworthy that most of these non-rectilinearly polarized waves correspond to late coda arrivals.

Fig. 5. An example of earthquakes analysed with ZLC and polarization techniques. From the top to the bottom of the figure are reported: Seismogram of the vertical component of station 1B filtered between 4 and 6 Hz. ZLC values plotted as a function of lapse time. Apparent slowness (and corresponding velocity, reported for clarity) calculated with the ZLC method for a time window of 50 points sliding of 30%. Values of the apparent velocity obtained for an average cross-correlations lower than 0.7 are excluded; the vertical lines No. 1 and No. 3 show the arrival of the first *P* and *S* pulses. See text for an explanation about line No. 2. The corresponding V_p/V_s ratio is close to 1.7. The same for back-azimuths. Plot of the parameter rectilinearity as a function of the lapse time. The same sliding window as the other plots was used. The same for angle β, that is the angle which the highest eigenvector forms with the vertical direction. The same for γ. γ is the angle between the wave vector direction and the direction of the eigenvector corresponding to the highest eigenvalue. For all the plots: the large black circles (rhombuses for apparent velocity) mark the points with a ZLC value greater than the threshold value of 0.7. The first black dot corresponds to the direct *P*-wave arrival.

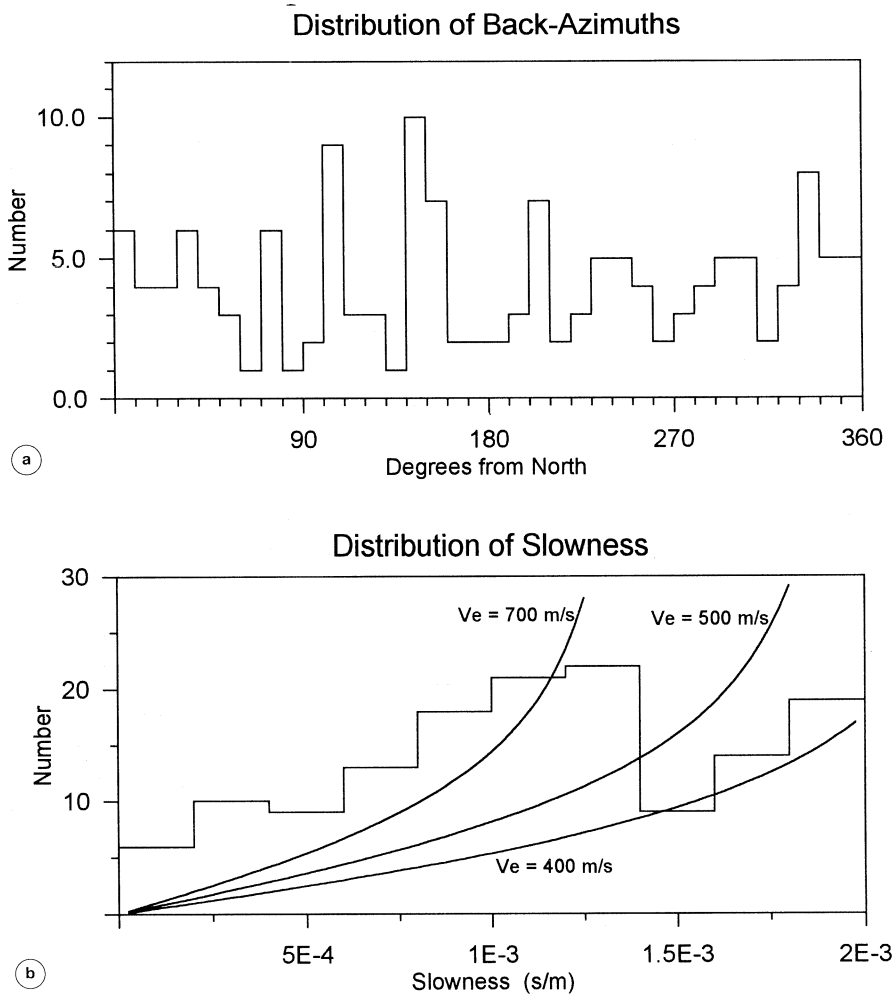

Fig. 6a,b. Total dstribution of back-azimuth (a) and slowness (b) obtained by the coda analysis for the seven events studied. In (b) the three lines correspond to the theoretical distribution of slowness in the case of uniform distribution of scatterers in uniform velocity earth media, characterized respectively by a velocity of 400, 500 and 700 m/s.

6. Data analysis and results for Deception volcano

A small aperture seismic array was deployed near the «Gabriel de Castilla» Spanish base on Deception Islands during the two Antarctic summers of 1994-1995 and 1995-1996. Configuration was the same for the two surveys (fig. 7). Sensors were the same as those utilized for Teide volcano. We recorded a total of about 600 seismic events during the first survey and more than 1000 in the second one. A detailed analysis is reported in a paper by Del Pezzo *et al.* (1997). In the present paper we will describe the results obtained analyzing the so-called hybrid events, showing a *P*-phase

followed by a second phase composed of Rayleigh waves, and a short duration coda following the second phase. These events are interpreted as generated by the presence of explosions in a shallow acquifer, generated by the volcanic activity.

We selected about 30 events on the basis of the best signal to noise ratio. The spectra of these signals show two distinct peaks (1-3 and 4-8 Hz). We filtered the data around the two main peaks of the spectrum, using a 5-pole Butterworth filter.

The width of the pass-band used depends on the width of the observed spectral peak. We determined visually for each event the bandwidth containing the most energy, centering it at the main peak obtaining a width range from 2 to 7 Hz. Then we applied the zero-lag cross-correlation method to the filtered seismograms in order to determine the apparent slowness across the array and the back-azimuth to the associated source. We used a moving window with a length in time domain which depends on the value of the lowest observed peak frequency in the filter band, in order to use always 2 periods in each window.

We started at the pre-event noise and stopped well into the coda. For each step we evaluated back-azimuth and slowness. Errors in azimuth were smaller than 10° and of the or-

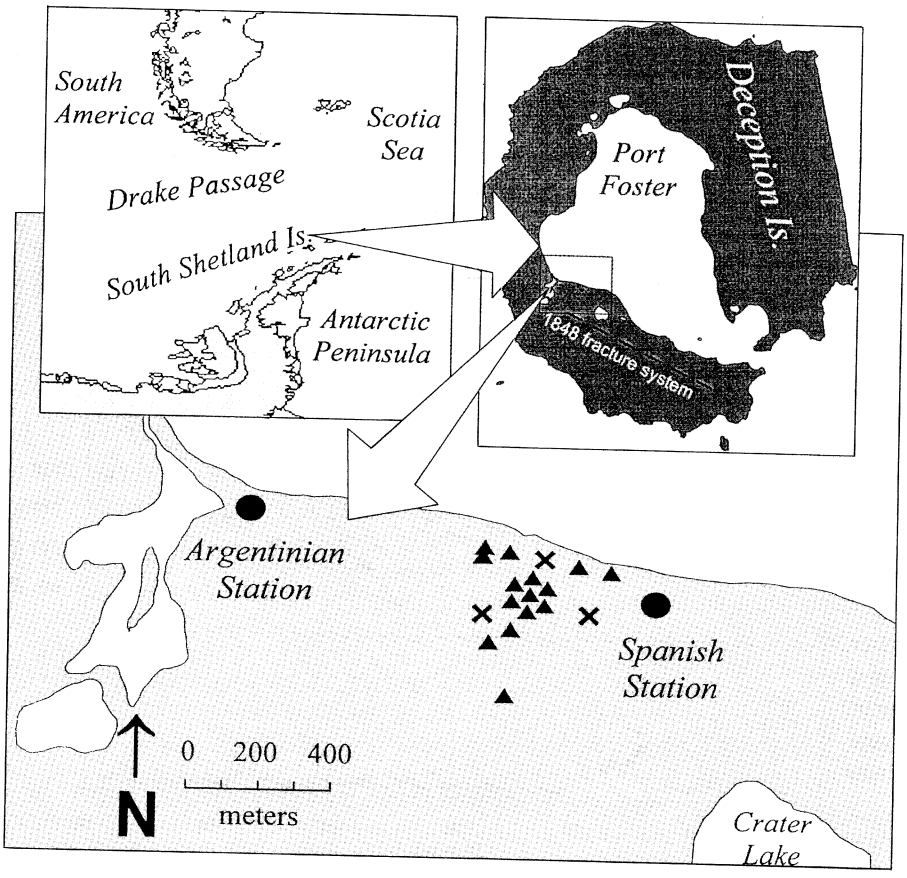

Fig. 7. Configuration of the seismic array installed on Deception Island (South Shetland, Antartica) composed of 15 vertical component sensors and three three-component sensors.

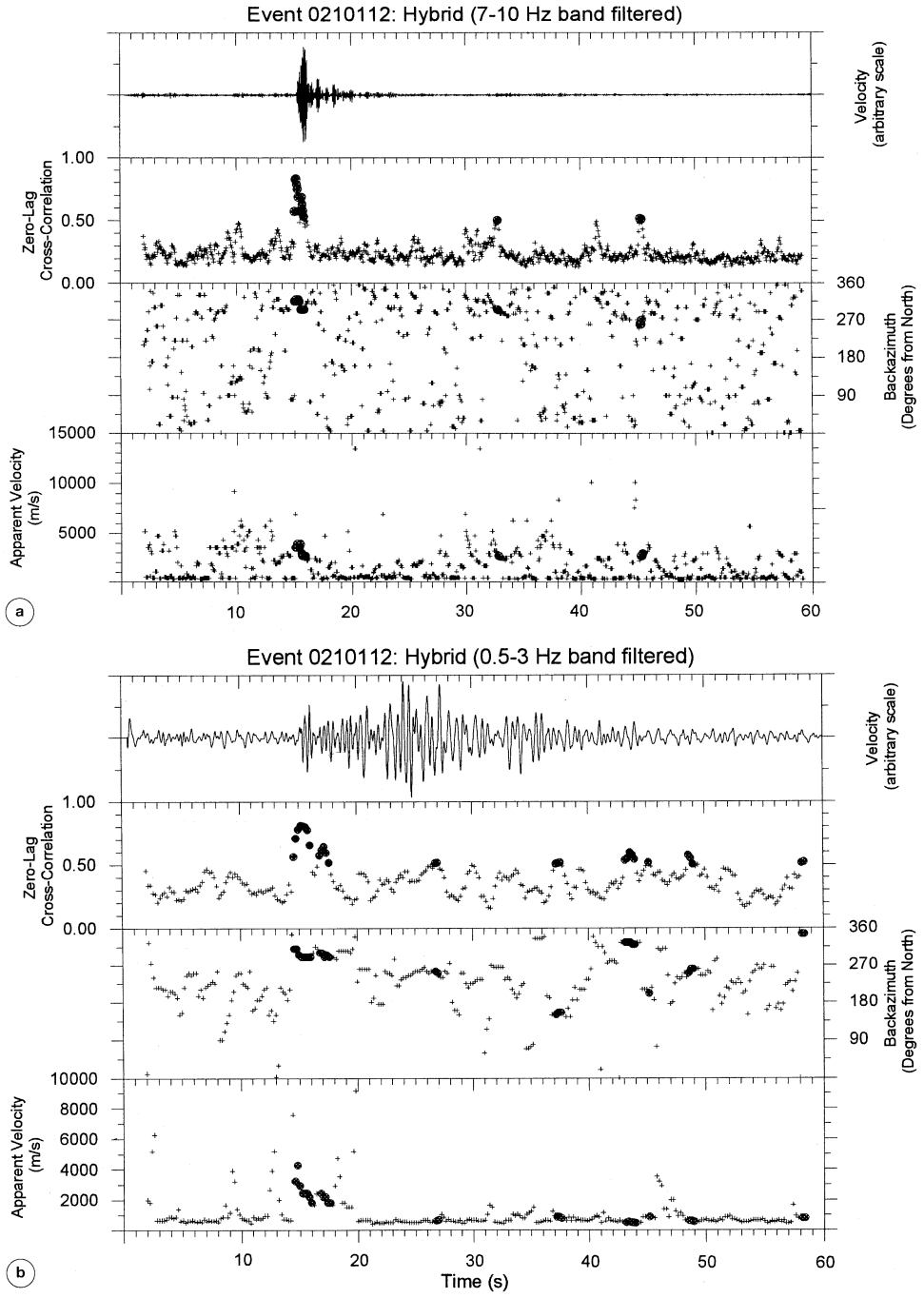

Fig. 8a,b. Hybrid event analysed with ZLC method. We report correlation value, back-azimuth and apparent velocity *vs.* lapse time for two frequency band: 7-10 Hz (a) and 0.5-3 Hz (b).

der of 10% in slowness for correlation higher than 0.7. An example of such analysis is reported in fig. 8a,b. The hybrid events show a high correlation for the first phase in the high frequency band, corresponding to apparent velocities up to about 4 km/s, and high correlation in the windows corresponding to the low frequency wave packet which follows the first phase. This last wave packet arrives at the array with low apparent velocity and with back-azimuth which are often different from that of the first phase.

We clearly observe that the high frequency phases have higher apparent velocity than the low frequency ones, and that the most signals come from the south-west sector. For hybrids, the high frequency phase comes from a direction slightly different from that of the low frequency phase, which as already described, appears some seconds later on the seismogram. This second phase could be produced by a strong scatterer, located near the source or the station.

A polarization analysis was carried out with the same method described above for Teide volcano. The results, not reported for brevity, show that the first phase is composed only of *P*-waves, while the longer period phase and the coda are composed of surface waves (mixed Rayleigh and Love waves types).

7. Discussion and conclusions

Data from Teide are a set of earthquakes with a location in a volcanic structure. Due to the appearance of their seismograms, and to the shape of their displacement spectra (not reported in the present paper) which were routinely carried out on the present data set, these events can be grouped into the category of the volcano-tectonic events (Power *et al.*, 1994), as they show a clear impulsive *P* and *S* phases, followed by a regularly decaying coda. Volcano-tectonic events share the same spectral shape as the tectonic earthquakes, with a flat low-frequency trend and a rapid high frequency decay, and are reasonably generated by an impulsive double couple source. The corner frequencies observed on our spectra are always greater than 6 Hz.

Due to this evidence, we could not expect focused energy in the early coda, due to a persistent source of seismic activity, as found for example by Goldstein and Chouet (1994) for tremor and Gas-piston events at Kilauea, or by Chouet *et al.* (1997) for explosion-quakes at Stromboli volcano, Italy. In the last two papers the array analysis was carried out on seismic events with a non-double couple and persistent source, directly generated by the volcanic activity.

In the present paper we selected for coda wave analysis the frequency band between 4 and 6 Hz. In this frequency range the best signal to noise ratio was observed for the available data. This band corresponds, moreover, to one of the most frequently analyzed frequency bands for the majority of the papers on coda waves reported in the literature (Aki, 1980). In our case the frequency band also corresponds to the highest signal energy. The analyzed frequency band limits the analysis to a heterogeneity scale, a, in the range from 2 to 200 m, hypothesizing large angle scattering phenomena for coda generation (Wu and Aki, 1988). As large angle scattering occurs for ka in the range 0.1-10 (k is the wave number), taking the velocity equal to the average velocity obtained from the array measurements (1000 m/s), we obtained an heterogeneity scale between 2 and 200 m.

The results on apparent velocity and back-azimuth measurements along the coda show that in the analyzed frequency band the coda of the seven short period earthquakes recorded at the array located on Teide active volcano is composed of waves which show almost no correlated arrivals, except for isolated arrivals with low apparent velocity (compared with the direct *S*-wave velocity) and random space distribution of back-azimuths. Nakamura (1977), analyzing the polarization properties of the moonquake coda waves, showed a decreasing coherence with increasing lapse time along the coda. These effects were interpreted by Nakamura (1977) as produced by multiple scattering phenomena.

Some authors show experimental evidence of strong scatterers in the earth medium located close to the seismic network, contributing to well correlated radiation in the coda

of local earthquakes (Furumoto *et al.*, 1990; Nishigami, 1991), superimposed on an uncorrelated (or random) background radiation. Using a deterministic approach to study this highly correlated part of coda, these authors are able to locate the sources of strong scattering. In the present paper a similar situation is present: the experimental results obtained can be interpreted as produced by a random distribution of scatterers on which localized strong scatterers are superimposed. The uncorrelated part may be produced by multiple scattering from randomly distributed heterogeneity, while the well correlated part may be generated by single scattering by strong scatterers.

Data show that many of the arrivals with the highest correlation in the early coda show apparent slowness close to the velocity of *S*-waves in the shallowest layers. This could indicate that some strong scatterers are localized, in the investigated zone, mostly near the surface and are possibly related to the strong irregularities in the topography, which is characterized by the presence of the Teide cone and the caldera borders surrounding the array site. Due to the limited number of events and to the spread distribution of the hypocentral distances we were unable to recognize definite combinations of apparent slowness and back-azimuth related to the position of strong scatterers. Their dimension in our analysis would not exceed some hundreds of meters, as already discussed. They could correspond to small topographic irregularities, or to zones with strong density contrast, like for example magma intrusions.

Many observations (see Aki, 1980) carried out on data sets obtained throughout the world show that coda waves seem to be composed mostly of *S*-waves, even though some contamination with Rayleigh and Love type surface waves seem to characterize the coda waves recorded at particular sites (for example in small basins, as discussed in Ibanez *et al.*, 1991 and Steck *et al.*, 1989). The *S* composition is also supported theoretically (Zeng, 1993). The polarization analysis carried out in the present paper shows that a high percentage of the uncorrelated part of the coda is linearly polarized (high rectilinearity). Moreover, the particle motion amplitude in the horizontal plane is higher than that in the vertical direction. This can be deduced from the β parameter which takes the highest values in the lapse time range corresponding to non-correlated arrivals.

The analysis of the wave composition of the well correlated wavetrains shows some arrivals with a *SH* type polarization (high β and γ, as for example the arrival at 29 s in fig. 3), while others seem to have a different polarization with intermediate values of β and γ, showing the possible presence of Rayleigh surface waves.

In the light of the present results we can reasonably exclude the hypothesis that in the investigated frequency band the early *S*-coda is produced by multiple *S*-wave arrivals propagating in a plane layered medium. In fact, we measured strong back-azimuth variation and constant apparent velocity for different time windows along the coda. The opposite would occur (almost constant back-azimuth and increasing apparent velocity with increasing lapse time) for multiple reverberation of an *S* phase in a layered earth structure.

The well correlated arrivals in the late coda could correspond to strong scatterers located at a distance of the order of 50 km from the array, in the hypothesis of single scattering. We cannot exclude that these arrivals could correspond to correlated noise bursts, superimposed on the coda radiation for seismogram windows with low signal to noise ratio, because, even if we never observed well correlated arrivals in the time window containing pure seismic noise, as shown in fig. 4, some (3%) of the ZLC values for pure noise are just below the threshold limit. We need further analysis applied to more energetic signals with longer codas, recorded in the same zone, to answer to this question.

Data from Deception Island are a set of volcanic events. They are generated by explosive sources and do not generate *S*-waves. The coda is short, composed mainly of surface waves and, differently from the coda of the volcano-tectonic events, shows arrivals with a constant back-azimuth. Interestingly, this direction does not coincide with the direction of the first arrival, showing a possible strong scatterer located between source and array. The physical process of coda formation is completely differ-

ent for the two examples reported in the present paper. We have, in fact, evidence of random scattering in the case of Teide volcano, while strong scattering, strongly focused in a precise direction, is present in the case of Deception Island. The main difference between the two cases is the *S*-wave generation, almost absent in the case of the volcanic events in Deception. All the coda radiation in this last case is composed of surface waves.

REFERENCES

AKI, K. (1973): Scattering of *P* Waves under the Montana Lasa, *J. Geophys. Res.*, **78** (8), 1334-1346.

AKI, K. (1980): Scattering and attenuation of shear-waves in the lithosphere, *J. Geophys. Res.*, **85**, 6496-6504.

AKI, K. (1995): Interrelation between fault zone structures and earthquake processes, *Pageoph*, **145** (3/4), 647-676.

AKI, K. and B. CHOUET (1975): Origin of coda waves: source, attenuation, and scattering effects, *J. Geophys. Res.*, **80**, 3322-3342.

ARANA, V. (1994): Report of the coordinator, in European Laboratory Volcanoes: Teide. Definition of the fine structure and plumbing system aimed at eruption prediction, hazard assessment and eruptive mechanisms understanding. Contract EV5V-CT93-0283. Progress Report, 93-94. European Commission, Directorate General XII, Science, Research and Development-Joint Research Centre, Bruxelles.

CHOUET, B., G. SACCOROTTI, P.B. DAWSON, G. DE LUCA, G. MILANA, M. MARTINI and R. SCARPA (1997): Source and path effects in the wavefields of tremor and explosions at Stromboli volcano, Italy, *J. Geophys. Res.* (in press).

DAINTY, A.M. and M.N. TOKSOZ (1990): Array analysis of seismic scattering, *Bull. Seism. Soc. Amer.*, **80**, 2242-2260.

DEL PEZZO, E., M. LA ROCCA and J. IBANEZ (1997): Observations of high frequency scattered waves using dense arrays at Teide volcano, *Bull. Seism. Soc. Am.* (in press).

DEL PEZZO, E. *et al.* (1997): Observations of volcanic earthquakes and tremor at Deception Island-Antarctica, *Ann. Geofis.* (submitted).

FRANKEL, A. and L. WENNERBERG (1987): Energy-flux model of seismic coda: separation of scattering and intrinsic attenuation, *Bull. Seism. Soc. Amer.*, **77**, 1223-1251.

FRANKEL, A., S. HOUGH, P. FRIBERG and R. BUSBY (1991): Observations of Loma Prieta aftershocks from a dense array in Sunnyvale, California, *Bull. Seism. Soc. Am.*, **80**, 1900-1922.

FURUMOTO, M., T. KUNITOMO, H. INOUE, I. YAMADA, K. YAMAOKA, A. IKAMI and Y. FUKAO (1990): Twin sources of high-frequency volcanic tremor of Isu-Oshima volcano, *Japan, Geophys. Res. Lett.*, **17**, 25-27.

GAGNEPAIN-BEYNEIX, J. (1987): Evidence of spatial variations of attenuation in the Western Pyrenean range, *Geophys. J. R. Astron. Soc.*, **89**, 681-704.

GOLDSTEIN, P. and B. CHOUET (1994): Array measurements and modeling of sources of shallow volcanic tremor at Kilauea Volcano, Hawaii, *J. Geophys. Res.*, **99**, 2637-2652.

GAO, L.S., N.N. BISWAS, L.C. LEE and K. AKI (1983): Effects of multiple scattering on coda waves in three-dimensional medium, *Pageoph*, **121**, 3-15.

HOSHIBA, M. (1994): Simulation of coda wave envelope in depth dependent scattering and absorption structure, *Geophys. Res. Lett.*, **21**, 2853-2856.

HOSHIBA, M. (1995): Estimation of nonisotropic scattering in western Japan using coda wave envelopes: application of a multiple nonisotropic model, *J. Geophys. Res.*, **100**, 645-657.

IBANEZ, J.M., J. MORALES, F. DE MIGUEL, F. VIDAL, G. ALGUACIL and A.M. POSADAS (1991): Effect of sedimentary basin on estimations of Q_c and Q_{Lg}, *Phys. Earth Planet. Inter.*, **66**, 244-252.

MONTALBETTI, J.F. and E.R. KANASEVICH (1970): Enhancement of teleseismic body phase with a polarization filter, *Geophys. J. R. Astron. Soc.*, **21**, 119-129.

MORI, J., J. FILSON, E. CRANSWICK, R. BORCHERDT, R. AMIRBEKIAN, V. AHARONIAN and L. HACHVERDIAN (1994): Measurements of *P* and *S* wave fronts from the dense three-dimensional array at Garni, Armenia, *Bull. Seism. Soc. Am.*, **84**, 1089-1096.

NAKAMURA, Y. (1977): Seismic energy transmission in an intensely scattering environment, *J Geophys. Res.*, **43**, 389-399.

NISHIGAMI, K. (1991): A new inversion method of coda waveforms to determine spatial distribution of coda scatterers in the crust and uppermost mantle, *Geophys. Res. Lett.*, **18**, 2225-2228.

POWER, J.A., J.C. LAHR, R.A. PAGE, B.A. CHOUET, C.D. STEPHENS, D.H. HARLOW, T.L. MURRAY and J.N. DAVIES (1994): Seismic evolution of the 1989-1990 eruption sequence of Redoubt Volcano, Alaska, *J. Volcanol. Geotherm. Res.*, **62**, 69-94.

SATO, H. (1977): Single isotropic scattering model including wave conversion, *J. Phys. Earth*, **25**, 163-176.

SPUDICH, P. and T. BOTSWICK (1987): Studies of the seismic coda using earthquakes cluster as a deeply buried seismograph array, *J. Geophys. Res.*, **92**, 10526-10546.

STECK, L., W.A. PROTHERO and J. SCHEIMER (1989): Site-dependent coda *Q* at Mono Craters, California, *Bull. Seism. Soc. Amer.*, **79** (5), 1559-1574.

VERNON, F.L., J. FLETCHER, L. CARROL, A. CHAVE and E. SEMBERA (1991): Coherence of seismic body waves from local events as measured by a small-aperture array, *J. Geophys. Res.*, **96** (B7), 11981-11996.

WU, R.S. and K. AKI (1985): Elastic wave scattering by a random medium, *J. Geophys. Res.*, **90**, 10261-10273.

WU, R.S. and K. AKI (1988): Seismic wave scattering in three dimensionally heterogeneous earth, *Pageoph*, **128** (1/2), 1-6.

ZENG, Y. (1993): Theory of scattered *P* and *S* waves energy in a random isotropic scattering medium, *Bull. Seism. Soc. Amer.*, **83**, 1264-1277.